Quantifying the rise of the Himalaya orogen and implications for the South Asian monsoon

Lin Ding[1]*, R.A. Spicer[2,3]*, Jian Yang[2]*, Qiang Xu[1], Fulong Cai[1], Shun Li[1], Qingzhou Lai[1], Houqi Wang[1], T.E.V. Spicer[2], Yahui Yue[1], A. Shukla[4], G. Srivastava[4], M. Ali Khan[5], S. Bera[5,6], and R. Mehrotra[4]

[1]Key Laboratory of Continental Collision and Plateau Uplift, Institute of Tibetan Plateau Research, and Center for Excellence in Tibetan Plateau Earth Sciences, Chinese Academy of Sciences, Beijing 100101, China
[2]State Key Laboratory of Systematic and Evolutionary Botany, Institute of Botany, Chinese Academy of Sciences, Beijing 100093, China
[3]School of Environment, Earth and Ecosystem Sciences, The Open University, Milton Keynes MK76AA, UK
[4]Birbal Sahni Institute of Palaeobotany, Lucknow 226007, India
[5]Centre of Advanced Study, Department of Botany, University of Calcutta, Kolkata 700019, India
[6]Department of Botany, Sidho-Kanho-Birsha University, Ranchi Road, Purulia-723104, India

ABSTRACT

We reconstruct the rise of a segment of the southern flank of the Himalaya-Tibet orogen, to the south of the Lhasa terrane, using a paleoaltimeter based on paleoenthalpy encoded in fossil leaves from two new assemblages in southern Tibet (Liuqu and Qiabulin) and four previously known floras from the Himalaya foreland basin. U-Pb dating of zircons constrains the Liuqu flora to the latest Paleocene (ca. 56 Ma) and the Qiabulin flora to the earliest Miocene (21–19 Ma). The proto-Himalaya grew slowly against a high (~4 km) proto–Tibetan Plateau from ~1 km in the late Paleocene to ~2.3 km at the beginning of the Miocene, and achieved at least ~5.5 km by ca. 15 Ma. Contrasting precipitation patterns between the Himalaya-Tibet edifice and the Himalaya foreland basin for the past ~56 m.y. show progressive drying across southern Tibet, seemingly linked to the uplift of the Himalaya orogen.

INTRODUCTION

Quantifying the rise of the Himalaya since the onset of the collision of India with Asia at ca. 55 ± 10 Ma (Wang et al., 2014) has proved challenging and controversial (Garzione et al., 2000; Spicer et al., 2003; Currie et al., 2005; Rowley and Currie, 2006; DeCelles et al., 2007; Saylor et al., 2009; Ding et al., 2014), spurred on by the idea that changes in surface height, area, and surface characteristics of the Himalaya orogen and Tibetan Plateau underpin South Asian and East Asian monsoon dynamics (Molnar et al., 1993; Boos and Kuang, 2010). Opinions differ on how the plateau evolved, but modeling suggests that an orographic high such as the Himalaya may be more important than the elevation and/or extent of the entire plateau in shaping modern South Asian monsoon circulation (Boos and Kuang, 2010). Understanding the coupling between tectonics and climate requires quantification of elevation history, but to date little is known about the rise of the proto-Himalaya, with almost all the paleoaltimetry of different parts of the Himalayan chain only showing that it was near its present elevation by the late Miocene (Garzione et al., 2000; Saylor et al., 2009; Gébelin et al., 2013). To reconstruct elevation and climate history, we use environmental signatures archived in fossil leaf form.

In woody dicot angiosperms, evolutionary selection has resulted in a genome capable of producing highly variable leaf architecture optimized to local climate, and globally leaf form is more strongly linked to climate than taxonomic affinity (Yang et al., 2015). Unsurprisingly then, leaf form encodes the numerous climate metrics characteristic of monsoons (Spicer et al., 2016) as well as moist enthalpy, an expression of both atmospheric temperature and moisture that varies with elevation (Forest et al., 1999).

Moist static energy (h) is the total specific energy content (per unit mass) of air (excluding kinetic energy, which is very small [<1%] except during hurricanes) and is made up of two components, moist enthalpy and potential energy:

$$h = H + gZ, \qquad (1)$$

where H is moist enthalpy and gZ is potential energy (g is acceleration due to gravity, a constant, and Z is elevation). As a parcel of air rises against a mountain slope, it gains potential energy and, because moist static energy is conserved, moist enthalpy decreases. It follows, therefore, that the difference in elevation between two locations is given by:

$$\Delta Z = \frac{\left(H_{low} - H_{high}\right)}{g}. \qquad (2)$$

The simplicity of this equation offers an attractive paleoaltimeter for obtaining surface elevation and was used to obtain the first quantitative mid-Miocene paleoelevation of southern Tibet (Spicer et al., 2003).

Here we introduce and date two fossil plant–bearing sedimentary sections along the Yarlung-Zangpo suture (YZS) yielding the Liuqu and Qiabulin paleofloras, which together with a previously published 15 m.y. paleoflora from the Namling Basin, south Lhasa terrane (Spicer et al., 2003; Khan et al., 2014), and four sea-level floras of similar ages from Himalaya foreland basin (Srivastava et al., 2012; Khan et al., 2014; Shukla et al., 2014) (Fig. 1) allow us to chart elevation and climate change along the southern flank of the Himalaya-Tibet orogen over the past ~56 m.y.

GEOLOGICAL CONTEXT

The mostly conglomeratic Liuqu Formation outcrops are restricted to an elongate area south of the YZS. We investigated three sections extending south-north across the conglomerate between the towns of Lhaze and Xigatze (Fig. 2). Plant megafossils (36 species, representative specimens of which are shown in Fig. DR1 in the GSA Data Repository[1]) were found in siltstone beds from the lower parts of the three measured sections (Fig. 2E). A tuffite sample ~80 m above the fossil layers from the nearby Xialu section has a concordia age of 59.3 ± 0.8 Ma, with the nine youngest zircons giving ages from 56.4 Ma to 61.4 Ma (Fig. DR2; Tables DR1 and DR2 in the Data Repository), similar to those of the youngest cluster of U-Pb ages of detrital zircons from the upper part of the Za

---

[1]GSA Data Repository item 2017055, description of leaf forms, geological background, U-Pb analytical methods and results, Figures DR1–DR7, and Tables DR1–DR5, is available online at www.geosociety.org /datarepository/2017 or on request from editing@ geosociety.org.

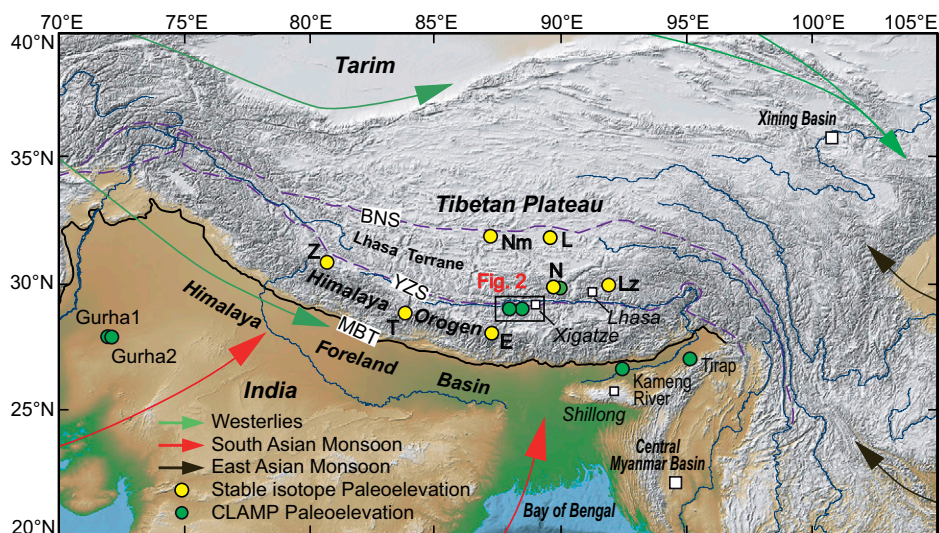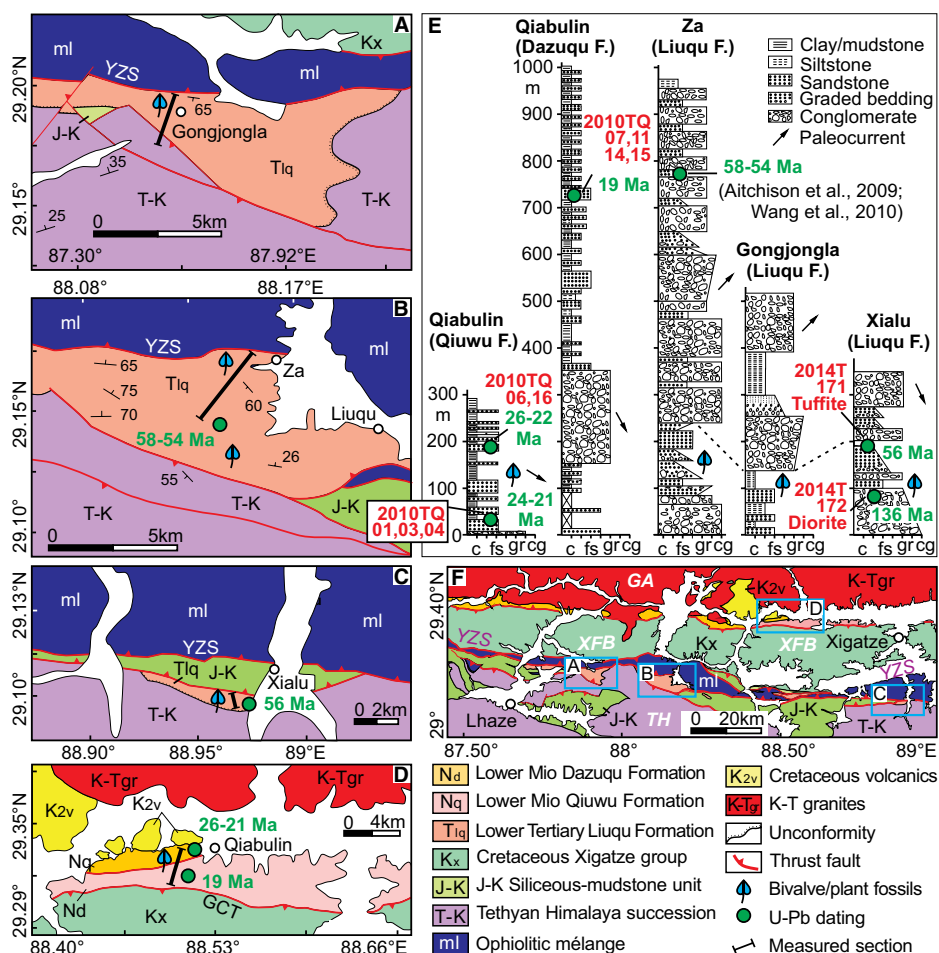*E-mails: dinglin@itpcas.ac.cn; r.a.spicer@open .ac.uk; yangjian@ibcas.ac.cn.

215

Figure 1. Sample locations in relation to major geological features in southern Himalaya-Tibet orogen. Paleoelevation study locations: Z—Zhada (~5.5–6.5 km elevation, 9.2 Ma; Saylor et al., 2009); T—Thakkhola (~5.5 km, 11–9 Ma; Garzione et al., 2000); E—Mount Everest (5.1–5.4 km, ca. 15 Ma; Gébelin et al., 2013); N—Namling (4.7–5.4 km, ca. 15 Ma; Spicer et al., 2003; Currie et al., 2005; Khan et al., 2014); Lz—Linzhou (4.5 km, ca. 60–54 Ma; Ding et al., 2014); Nm—Nima (4.6 km, ca. 26 Ma; DeCelles et al., 2007); L—Lunpola (4.8 km, ca. 40–35 Ma; Rowley and Currie, 2006). The Eocene (Gurha1 and Gurha2), late Oligocene (Tirap), and middle Miocene (Kameng River) Indian fossil floras (Srivastava et al., 2012; Khan et al., 2014; Shukla et al., 2014) are from low elevations (<300 m). CLAMP—Climate Leaf Analysis Multivariate Program (Spicer et al., 2003; http://clamp.ibcas.ac.cn); BNS—Bangong-Nujiang suture; YZS—Yarlung-Zangpo suture; MBT—Main Boundary thrust.

Figure 2. Map showing tectonic units and Cenozoic sediments in Himalaya-Tibet orogen. A–D: Geological map of Gongjiongla, Za, Xialu, and Qiabulin areas, respectively. YZS—Yarlung-Zangpo suture; GCT—Great Counter thrust. E: Lithostratigraphy of Liuqu, Qiuwu, and Dazuqu Formations. Grain Size: c—clay; fs—fine sandstone; gr—granule; cg—conglomerate. F: Geological map of Yarlung-Zangpo region between Lhaze and Xigatze towns. GA—Gangdese arc; XFB—Xigatze forearc basin; TH—Tethyan Himalaya. Unit ages: N—Neogene; T—Tertiary; K—Cretaceous; J—Jurassic; Mio—Miocene.

section, which range between 54 and 58 Ma (Fig. DR3; Table DR1). This constrains the deposition of the Liuqu floras to the latest Paleocene (ca. 56 Ma) and is in agreement with megafossil age estimations (Fang et al., 2005). In addition, U-Pb zircon ages of diorite clasts from the lower part of the Liuqu Formation range between 96 and 210 Ma (Fig. DR4; Table DR1) and are within the age range of Gangdese magmatic zircons but significantly different from Himalayan age patterns (Wang et al., 2010). This shows that the base of the Liuqu Formation was derived from the Gangdese arc.

The Qiabulin paleoflora (Fig. DR5) occurs in cross-bedded sandstones within 270 m of gray interlayered sandstones, mudstones, and thinly bedded coals of the Qiuwu Formation. The maximum age of the Qiuwu Formation is 26–21 Ma given by the youngest U-Pb ages of detrital zircons (Fig. 2E; Fig. DR3). The age of the overlying Dazuqu Formation is no older than ca. 19 Ma (Fig. 2E; Fig. DR3), as determined by U-Pb ages of detrital zircons and $^{40}Ar/^{39}Ar$ analyses of laterally equivalent tuffs (Aitchison et al., 2009), so the age of the Qiabulin flora has to be 21–19 Ma (Fig. 2D).

ESTIMATED PALEOELEVATIONS

The contrasting floral compositions indicate, qualitatively, substantial elevation differences. The ca. 56 Ma Liuqu flora reflects tropical and subtropical vegetation, including palms (Fig. DR6), similar to other contemporary near-sea-level floras in India and southern China (Shukla et al., 2014; Spicer et al., 2016). The earliest Miocene Qiabulin flora conspicuously lacks palms, is temperate in composition, and is distinct from the palm-rich tropical near-coeval coastal vegetation of northern India (Srivastava et al., 2012). The Namling flora is cool temperate in composition, characterized by *Alnus*, *Salix*, and *Acer* (Spicer et al., 2003; Khan et al., 2014), and must have been much higher in elevation than the sea-level mid-Miocene Kameng River flora of the Siwaliks, which is rich in tropical taxa such as *Dipterocarpus* and *Terminalia*. (Khan et al., 2014).

To quantify the elevation changes suggested by floral compositions, we analyzed leaf form.

The well-archived leaf fossils in the Liuqu and Qiabulin floras allow the use of the Climate Leaf Analysis Multivariate Program (CLAMP) (Spicer et al., 2003; http://clamp.ibcas.ac.cn) (Fig. 3; Tables DR3 and DR4), a non-taxonomic multivariate technique that derives paleoclimate, including paleoenthalpy, from fossil leaf form (e.g., Khan et al., 2014; Spicer et al., 2003).

Laterally equivalent marine units or the presence of mangrove remains show that fossil floras of early Eocene (assemblages Gurha1 and Gurha2), late Oligocene (Tirap), and mid-Miocene (Kameng River) (Fig. 1) age were deposited at sea level (Shukla et al., 2014; Srivastava et al., 2012; Khan et al., 2014). These provide past values of moist enthalpy at sea level (MESL) allowing us to determine the absolute paleoelevations of the Tibetan floras. Figure 3A shows that MESL stays within very narrow limits (353–357 kJ/kg) from ca. 53 Ma to 13 Ma, eliminating the need for precise age determination for the sea-level floras.

Because MESL varies somewhat across latitude, we used paleospatial trends in MESL derived from general circulation paleoclimate models (Fig. DR7) to correct for paleospatial differences between the fossil sites. To obtain MESL at the paleopositions of the Tibetan sites compatible with those obtained from leaf form, we used the modeled MESL differences between the Indian and Tibetan sites to adjust the CLAMP-derived MESL values obtained from the Indian floras (Table DR5). In practice we found that adjusted Liuqu and Qiabulin MESL values resulted in only small elevation increases (Fig. 4) well within methodological uncertainties of ±0.9 km.

Figure 3A also shows that the Liuqu flora plots close to the sea-level group, while the Qiabulin and Namling floras yield lower enthalpies indicating higher altitudes. Figures 3B and 3C and Table DR4 give all CLAMP results and show progressive drying on the Himalaya-Tibet orogen. Figure 4 and Table DR5 show predicted elevations of ~0.9 ± 0.9 km for the Liuqu fossil flora and ~2.3 ± 0.9 km for the Qiabulin leaves. As with previous results, the Namling Basin is predicted to have been at ~5.5 ± 0.9 km (Khan et al., 2014), ~1.2 km higher than the present-day basin floor.

DISCUSSION AND CONCLUSIONS

Building the Himalaya Orogen

Our CLAMP results, coupled with those using stable isotopes (Garzione et al., 2000; Saylor et al., 2009; Gébelin et al., 2013), place bounds on the surface uplift history of the Himalaya orogen (Fig. 4). Our study areas straddle the YZS and lie within the wedge-top depozone of the Yarlung-Zangpo foreland basin system which may have resulted from flexural subsidence when Asia loaded onto India. Between ca.
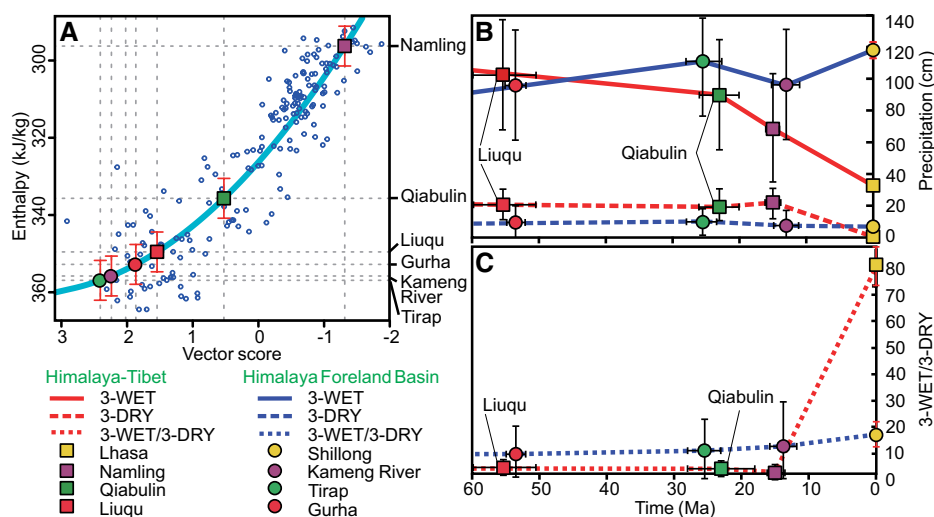

Figure 3. Plots of Climate Leaf Analysis Multivariate Program (CLAMP) results for Himalaya-Tibet orogen and Himalaya foreland basin (see Fig. 1 for sample locations). A: Enthalpy regression using PhysgAsia2 (http://clamp.ibcas.ac.cn/CLAMP_PhysgAsia2.html) and HiRes-GRIDMetAsia2 training sets (Khan et al., 2014). Error bars are 2σ. B: Comparison of precipitation during the three consecutive wettest months (3-WET) and three consecutive driest months (3-DRY) between Himalaya-Tibet orogen and Himalaya foreland basin. C: Ratio of 3-WET to 3-DRY gives indication of seasonality of rainfall.
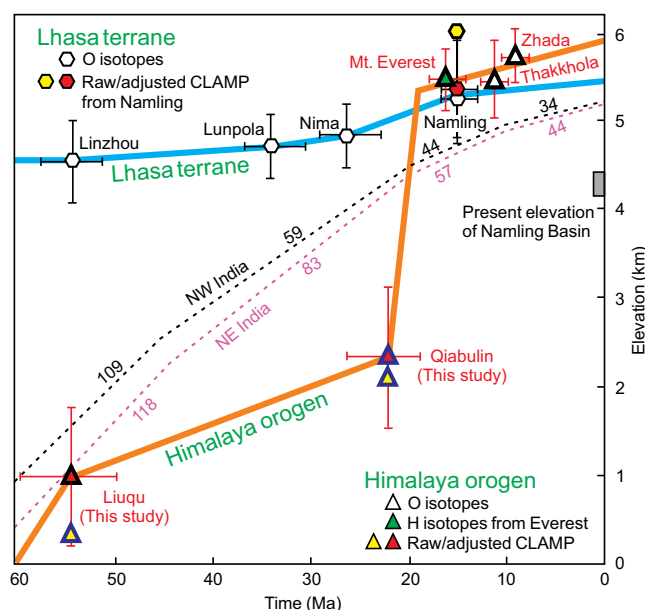

Figure 4. Time-altitude plot for Himalaya orogen based on Climate Leaf Analysis Multivariate Program (CLAMP) analysis and isotopes. Elevations are for basin floors (see Fig. 1 for locations); uncertainties are 2σ. Raw CLAMP elevations (yellow) are adjusted for model-derived latitude and longitude enthalpy gradients (red) (Khan et al., 2014). Dashed lines show average convergence rates (mm yr⁻¹) between India and Eurasia in the northwest and northeast corners of India since 60 Ma (Molnar and Stock, 2009).

58.5 Ma and ca. 55 Ma, the YZS must have been near sea level because the last marine units in the area are of this age (Ding et al., 2005) and was situated on the southern margin of the pre-existing high Gangdese Mountains (4.5 ± 0.4 km) (Ding et al., 2014).

CLAMP results and the distinctly tropical aspect of the palm-rich vegetation show that the Liuqu flora was still relatively low in elevation (~1 km or lower) soon after deposition of the last marine units. At the start of the Miocene, the Qiabulin flora was at ~2.3 km. By 15 Ma, stable isotope results put the Mount Everest region of the Himalaya at >5.0 km (Gébelin et al., 2013), similar to the elevation of Namling,

probably due to activation of southward thrusts and crustal thickening. Comparison of our uplift record with a 40% slowdown in the convergence rate between India and Asia during 20–11 Ma (Molnar and Stock, 2009) suggests that our localized paleoelevation history reflects uplift, and convergence resistance, on a wider scale along the southern flank of Tibet (Fig. 4), but our data do not constrain the many possible mechanisms involved.

Deformation and uplift were not transmitted as far north as the Namling Basin after 15 Ma. The minimum ~1 km descent of Namling since 15 Ma, due to extension along a north-south rift zone (Armijo et al., 1986), contrasts

with the modern high Himalaya, as typified by Mount Everest, which has been maintained >5.0 km over the last 15 m.y. (Gébelin et al., 2013). Thus, we propose that the present high Himalaya could be the most recent expression of a southward-migrating locus of crustal compression and mountain building, north of which gravitational collapse and east-west extension resulted in subsidence.

South Asian Monsoon Implications

Early Eocene (ca. 55–52 Ma) leaves from Gurha, India (Fig. 1), indicate a strong seasonal rainfall contrast (Figs. 3B and 3C) typical of a monsoon system (Shukla et al., 2014) but distinct in character from that of the present South Asian monsoon (Spicer et al., 2016). At low paleolatitudes (<10°), this seasonality is produced by migrations of the Intertropical Convergence Zone (ITCZ), but other evidence of late Paleocene to early Eocene rainfall seasonality poleward of the ITCZ migrational range (Licht et al. 2014), including the variations of $\delta^{18}O$ values in ostracods in the high Gangdese Mountains (Ding et al., 2014), suggests that the proto–Tibetan Plateau, including the Gangdese Mountains, played a role in shaping the late Paleocene–early Eocene South Asian monsoon. Our data show there has been a persistence of monsoon-like rainfall seasonality to the south of the Himalaya-Tibet edifice since the Paleogene (Figs. 3B and 3C).

The amount of precipitation during the three consecutive wettest months just north of the present Himalaya gradually decreased from 103 cm in the late Paleocene, through 90 cm in the earliest Miocene, to 68 cm in the middle Miocene, and to the present 33 cm at Lhasa (Figs. 3B and 3C). One likely cause is the "rainout" effect from northward-moving moist air on encountering the Himalaya, while another is deflection of the moist air to the east. This drying is most acute in the wet (summer) season when northward airflow is strongest. In contrast, the low-altitude sites to the south of the Himalaya-Tibet orogen show that summer rainfall has remained in a relatively stable range between 96 cm and 118 cm since ca. 56 Ma. Southern Tibet in the Miocene was wetter than seen today as shown by the presence of mid-Miocene cool temperate woodland inferred from the Namling fossils (Khan et al., 2014; Spicer et al., 2003). Since 15 Ma, the southern Tibetan Plateau has dried markedly, and we speculate that it was predominantly the Himalaya projecting above the Tibetan Plateau, rather than the area of plateau exceeding 4 km, that gave rise to this drying, consistent with the modeling results of Boos and Kuang (2010) who suggested that the Himalaya, rather than the Tibetan Plateau, exerts a strong orographic influence on South Asian monsoon circulation.

Our study provides proxy quantitative paleoaltimetry for the development of the modern Himalaya orogen, which rose against a preexisting proto–Tibetan Plateau when India began its collision with Asia. As collision progressed, the Himalayan crest developed southward, and as it projected above the Tibetan Plateau, produced progressive drying and eventually gave rise to the modern South Asian monsoon.

REFERENCES CITED
Aitchison, J.C., Ali, J.R., Chan, A., Davis, A.M., and Lo, C.H., 2009, Tectonic implications of felsic tuffs within the Lower Miocene Gangrinboche conglomerates, southern Tibet: Journal of Asian Earth Sciences, v. 34, p. 287–297, doi:10.1016/j.jseaes.2008.05.008.

Armijo, R., Tapponnier, P., Mercier, J.L., and Han, T.L., 1986, Quaternary extension in southern Tibet: Field observations and tectonic implications: Journal of Geophysical Research, v. 91, p. 13,803–13,872, doi:10.1029/JB091iB14p13803.

Boos, W.R., and Kuang, Z., 2010, Dominant control of the South Asian monsoon by orographic insulation versus plateau heating: Nature, v. 463, p. 218–222, doi:10.1038/nature08707.

Currie, B.S., Rowley, D.B., and Tabor, N.J., 2005, Middle Miocene paleoaltimetry of southern Tibet: Implications for the role of mantle thickening and delamination in the Himalayan orogen: Geology, v. 33, p. 181–184, doi:10.1130/G21170.1.

DeCelles, P.G., Quade, J., Kapp, P., Fan, M., Dettman, D.L., and Ding, L., 2007, High and dry in central Tibet during the Late Oligocene: Earth and Planetary Science Letters, v. 253, p. 389–401, doi:10.1016/j.epsl.2006.11.001.

Ding, L., Kapp, P., and Wan, X., 2005, Paleocene–Eocene record of ophiolite obduction and initial India-Asia collision, south central Tibet: Tectonics, v. 24, TC3001, doi:10.1029/2004TC001729.

Ding, L., Xu, Q., Yue, Y., Wang, H., Cai, F., and Li, S., 2014, The Andean-type Gangdese Mountains: Paleoelevation record from the Paleocene–Eocene Linzhou Basin: Earth and Planetary Science Letters, v. 392, p. 250–264, doi:10.1016/j.epsl.2014.01.045.

Fang, A.M., Yan, Z., Liu, X.H., Pan, Y.S., and Li, J.L., 2005, The flora of the Liuqu formation in South Tibet and its climate implications: Acta Micropalaeontologica Sinica, v. 44, p. 435–445.

Forest, C.E., Wolf, J.A., and Emanuel, K.A., 1999, Palaeoaltimetry incorporating atmospheric physics and botanical estimates of paleoclimate: Geological Society of America Bulletin, v. 111, p. 497–511, doi:10.1130/0016-7606(1999)111<0497:PIAPAB>2.3.CO;2.

Garzione, C.N., Quade, J., DeCelles, P.G., and English, N.B., 2000, Predicting paleoelevation of Tibet and the Himalaya from $\delta^{18}O$ vs. altitude gradients in meteoric water across the Nepal Himalaya: Earth and Planetary Science Letters, v. 183, p. 215–229, doi:10.1016/S0012-821X(00)00252-1.

Gébelin, A., Mulch, A., Teyssier, C., Jessup, M.J., Law, R.D., and Brunel, M., 2013, The Miocene elevation of Mount Everest: Geology, v. 41, p. 799–802, doi:10.1130/G34331.1.

Khan, M.A., Spicer, R.A., Bera, S., Ghosh, R., Yang, J., Spicer, T.E.V., Guo, S.X., Su, T., Jacques, F., and Grote, P.J., 2014, Miocene to Pleistocene floras and climate of the Eastern Himalayan Siwaliks, and new palaeoelevation estimates for the Namling-Oiyug Basin, Tibet: Global and Planetary Change, v. 113, p. 1–10, doi:10.1016/j.gloplacha.2013.12.003.

Licht, A., et al., 2014, Asian monsoons in a late Eocene greenhouse world: Nature, v. 513, p. 501–506, doi:10.1038/nature13704.

Molnar, P., and Stock, J.M., 2009, Slowing of India's convergence with Eurasia since 20 Ma and its implications for Tibetan mantle dynamics: Tectonics, v. 28, TC3001, doi:10.1029/2008TC002271.

Molnar, P., England, P., and Martinod, P.J., 1993, Mantle dynamics, uplift of the Tibetan Plateau, and the Indian monsoon: Reviews of Geophysics, v. 31, p. 357–396, doi:10.1029/93RG02030.

Rowley, D.B., and Currie, B.S., 2006, Palaeo-altimetry of the late Eocene to Miocene Lunpola basin, central Tibet: Nature, v. 439, p. 677–681, doi:10.1038/nature04506.

Saylor, J.E., Quade, J., Dellman, D.L., DeCelles, P.G., Kapp, P.A., and Ding, L., 2009, The late Miocene through present paleoelevation history of southwestern Tibet: American Journal of Science, v. 309, p. 1–42, doi:10.2475/01.2009.01.

Shukla, A., Mehrotra, R.C., Spicer, R.A., Spicer, T.E.V., and Kumar, M., 2014, Cool equatorial terrestrial temperatures and the South Asian monsoon in the Early Eocene: Evidence from the Gurha Mine, Rajasthan, India: Palaeogeography, Palaeoclimatology, Palaeoecology, v. 412, p. 187–198, doi:10.1016/j.palaeo.2014.08.004.

Spicer, R.A., Harris, N.B.W., Widdowson, M., Herman, A.B., Guo, S.X., Valdes, P.J., Wolfe, J.A., and Kelley, S.P., 2003, Constant elevation of southern Tibet over the past 15 million years: Nature, v. 421, p. 622–624, doi:10.1038/nature01356.

Spicer, R.A., Yang, J., Herman, A.B., Kodrul, T., Maslova, N., Spicer, T.E.V., Aleksandrova, G., and Jin, J., 2016, Asian Eocene monsoons as revealed by leaf architectural signatures: Earth and Planetary Science Letters, v. 449, p. 61–68, doi:10.1016/j.epsl.2016.05.036.

Srivastava, G., Spicer, R.A., Spicer, T.E.V., Yang, J., Kumar, M., Mehrotra, R., and Mehrotra, N., 2012, Megaflora and palaeoclimate of a late Oligocene tropical delta, Makum Coalfield, Assam: Evidence for the early development of the South Asia Monsoon: Palaeogeography, Palaeoclimatology, Palaeoecology, v. 342, p. 130–142, doi:10.1016/j.palaeo.2012.05.002.

Wang, C., Dai, J., Zhao, X., Li, Y., Graham, S.A., He, D., Ran, B., and Meng, J., 2014, Outward-growth of the Tibet Plateau during the Cenozoic: A review: Tectonophysics, v. 621, p. 1–43, doi:10.1016/j.tecto.2014.01.036.

Wang, J.G., Hu, X.M., Wu, F.Y., and Jansa, L., 2010, Provenance of the Liuqu Conglomerate in southern Tibet: A Paleogene erosional record of the Himalayan-Tibetan orogen: Sedimentary Geology, v. 231, p. 74–84, doi:10.1016/j.sedgeo.2010.09.004.

Yang, J., et al., 2015, Leaf form–climate relationships on the global stage: An ensemble of characters: Global Ecology and Biogeography, v. 24, p. 1113–1125, doi:10.1111/geb.12334.